

Analysing the Operating Limits in High Gravity Equipment

Kai Groß*, Kolja Neumann, Mirko Skiborowski, Andrzej Górak

TU Dortmund University, Laboratory of Fluid Separations, Emil-Figge-Straße 70, 44227 Dortmund, Germany
kai.gross@tu-dortmund.de

The enhancement of gas-liquid mass transfer is one of the key challenges in chemical separation processes. So far, gas-liquid contacting is predominantly performed in counter-currently operated conventional columns. However, economic and environmental constraints require continuous process improvement in terms of separation efficiency and capacity. Therefore, new column internals have been developed for conventional columns allowing for increased throughput at high performance (Spiegel and Duss, 2014). A fundamentally different approach to increase the hydraulic capacity in contacting equipment is to superimpose the gravitational force by applying a centrifugal force.

To realize this approach a ring shaped packing is mounted on a rotating shaft in a so-called rotating packed bed (RPB). By application of centrifugal forces, 10-1000 times higher than the gravitational force, a capacity increase is achieved. Although the increased throughput comes at the price of an elevated pressure drop and additional power consumption of the rotating equipment, it provides a great potential for debottlenecking of existing processes or implementing gas-liquid separation technologies in space limited environment and mobile environments, like off-shore applications. Furthermore, the rotational speed acts as an additional degree of freedom for an RPB, which provides additional flexibility in terms of applicable operational conditions. Besides the height of a packing and the specific packing material, recent studies by Neumann et al. have shown that also the type of nozzle for the distribution of the liquid in the eye of the rotor is of significant importance for the specific operating limits of an RPB. Therefore, the right choice of a nozzle design can facilitate a significant higher hydraulic capacity (Neumann et al., 2017a).

In the present study, we investigate the operating limits with liquid loads, at the inner cross-sectional area, up to $320 \text{ m}^3 \text{ m}^{-2} \text{ h}^{-1}$ and a F-factor of $4 \text{ Pa}^{0.5}$. We provide detailed insights on the relationship between the pressure drop and the rotational speed and elucidate which rotational speed is needed to achieve a certain capacity for the equipment.

1. Introduction

The operation of conventional columns for gas liquid contacting is limited by the different forces acting on the down flowing liquid. On the one hand, there is the gravitational force which drives liquid films, droplets or rivulets downwards the column. On the other hand, there are frictional forces between gas and liquid which are driving the liquid in the opposite direction. If the applied gas load to the column exceeds a certain limit a slight increase in pressure drop and liquid hold up becomes recognizable. As a consequence this limit is called loading point. Column operation above this point enables a very good separation efficiency. If the gas load increases further the so-called flooding point is passed, at which the maximum hydraulic capacity is reached, which eventually leads to an inoperability of the equipment. (Düssel et al., 2006, p. 760)

Due to this limitation conventional columns are very seldom operated above liquid loads of $100 \text{ m}^3 \text{ m}^{-2} \text{ h}^{-1}$ and a gas capacity factor over $2 \text{ Pa}^{0.5}$ at the same time (Yildirim et al., 2015). Rotating packed beds (RPBs) can be operated at higher loads because the centrifugal force exceeds the aforementioned gravitational force by far, shifting the correlation of forces. Moreover, due to the operational flexibility it is possible to operate close to the maximum hydraulic capacity at different liquid loads. In case liquid entrainment occurs during operation, the centrifugal force can be increased by an adjusted rotational speed.

2. Theoretical background

The hydrodynamic characteristics of conventional columns and RPBs are comparable. Nevertheless there are significant differences in the geometrical dimensions. For the operating limit of a conventional column two main design parameters are important. The cross sectional area $A_{C,column}$, which is limiting the maximum gas and liquid of the column, is determined by the column diameter/radius r_{column} . Additionally the height h_{column} is an important factor, because it determines the maximal separation efficiency which can be achieved in the equipment. In contrast to a column, in which gas and liquid flow bottom-up or top-down, respectively, the flow direction in the RPB is from the inner radius to the outer radius or vice versa, as a consequence the effect of the characteristic parameters changes. As the height of the column h_{column} , the radius of the rotor r_{RPB} determines the separation efficiency for an RPB, while the axial packing height h_{RPB} is important for the maximum capacity of an RPB, just as the radius of the column r_{column} . While the cross sectional area is constant in a conventional column, it is function of the radius in a RPB, more precise the values of the specific loads change along with the radius.

$$A_{C,column} = \pi r_{column}^2 \sim r_{column}^2 = const. \quad (1)$$

$$A_{C,RPB} = 2\pi h_{RPB} r_{RPB} \sim r_{RPB} = f(r) \quad (2)$$

Due to the difference in the geometrical dimensions, RPBs and columns are not directly comparable.

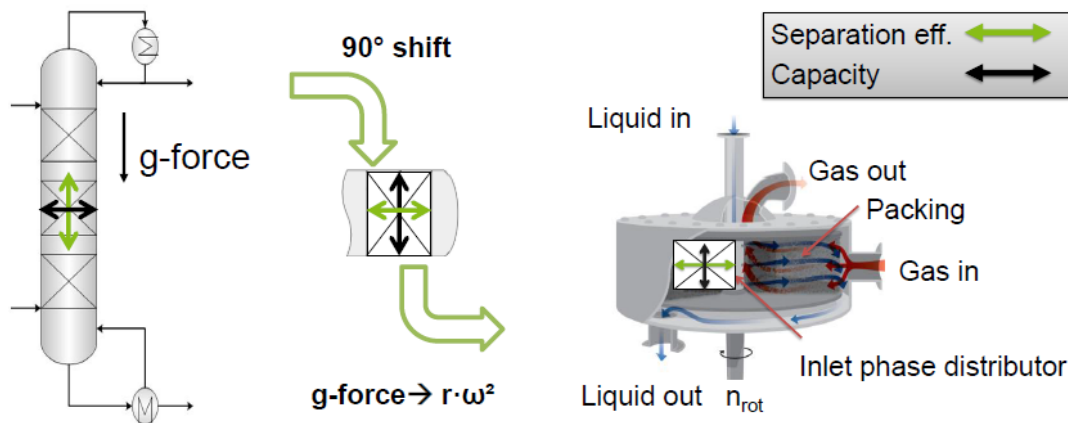


Figure 1: Schematic comparison between conventional column and rotating packed bed.

One way to compare different types of equipment is to use specific liquid loads LL and the gas capacity factor F_G . As previously explained they can be assumed nearly constant along the height in a conventional column, while these loads change along the rotor with the radius for an RPB. For hydrodynamic investigations the smallest cross sectional area is at the inner radius of the packing, hence it is reasonable to assume that the first liquid entrainment will occur at this position. In this work therefore the maximum operating limit will always be related to the loads at the inner radius of the packing LL_i or $F_{G,i}$.

$$LL = \frac{\dot{V}_L}{A_c(r)} \quad (3)$$

$$F_G = \frac{\dot{V}_G}{A_c(r)} \sqrt{\rho_G} \quad (4)$$

3. Material and methods

3.1 Experimental setup

In the current study a single stage RPB was investigated. The rotor had an inner diameter of 146 mm and an outer diameter of 500 mm. The axial packing height was 10 mm. A stainless steel knit mesh packing was used, it was wound around the inner eye ring of the rotor and its porosity ϵ of 0.83 was determined by weighing the packing. Due to rotor spacers for the upper and lower rotor plate the packing was limited to an outer diameter of 460 mm. For the liquid distribution a 360° pipe distributor was used which had two rows of 24 evenly spaced 1.1 mm holes (Figure 2). Gas and liquid flows were measured with flowmeters from the company Kobold. The thermal flow meter for the gas flow has in the investigated range a maximal error of $1.2 \text{ m}_{\text{norm}}^3 \text{ h}^{-1}$, while the absolute measurement accuracy of the turbine flow meter is $0.036 \text{ m}^3 \text{ h}^{-1}$. For the measurement of the pressure drop a glas u-tube manometer was used. The accuracy can be estimated to around 15 Pa.

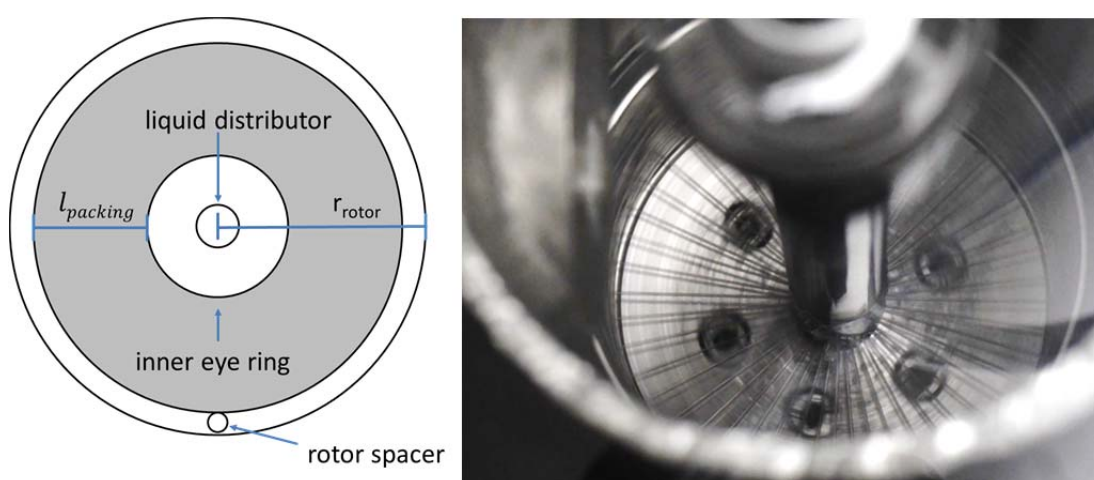


Figure 2: Schematic drawing of a rotor and photograph of the pipe distributor in the center of the RPB

3.2 Experimental procedure

Water and air were used at ambient conditions in order to investigate the operating limits, different process parameters were varied. These parameters were LL , F_G and n_{rot} . Always only one of the parameters at a time was varied. The liquid flow rate was varied between 0.36 and $1.5 \text{ m}^3 \text{ h}^{-1}$ which corresponds to a LL_i of 77 to $327 \text{ m}^3 \text{ m}^2 \text{ h}$. The range of the gas flow was modified between 15 and $60 \text{ m}_{\text{norm}}^3 \text{ h}^{-1}$ corresponding to a $F_{G,i}$ of 1 to $4 \text{ Pa}^{0.5}$. The rotational speed was varied between 0 and 30 s^{-1} . Two methods (A&B) were used to determine the maximal operating limit. They are briefly summarized in the following, while a more detailed description can be found in the article of (Neumann et al., 2017a).

In Method A the rotational speed was set to 30 s^{-1} . When this rotational speed was reached, the gas and liquid streams were injected. When all flow rates were constant and the measured pressure drop across the rotor was not changing steady state was assumed and in the next step the rotational speed was reduced. For smaller flow up to $0.72 \text{ m}^3 \text{ h}^{-1}$ the rotation was stopped, while at larger flow rates due to the significant entrainment of liquid with the gas it could only be reduced to a point where operation was still possible. In Method B the rotational speed and the liquid flow rate was set to a constant value while the gas flow rate was increased from 0 to $60 \text{ m}_{\text{norm}}^3 \text{ h}^{-1}$ with a step size of $5 \text{ m}_{\text{norm}}^3 \text{ h}^{-1}$. To ensure the quality of the experiment, the measurement procedure was repeated especially for points close to the maximum operating limit. This maximum operating limit was reached when the liquid was significantly entrained with the gas through the gas outlet. Measurements with lower rotational speeds using Method A were not considered for evaluation, since most of the liquid is entrained and has either no or only marginal contact to the packing.

4. Results and discussion

The performed hydrodynamic experiments can be interpreted in two different ways. First, one can generate a pressure drop curve which shows a characteristic trend (Figure 3 a). Starting with a moderate pressure drop at a high rotational speed, the pressure drop decreases with the reduction of the rotational speed. Around 15 s^{-1}

a minimum is reached. It can be assumed that the pressure drop is decreasing because the rotor and packing create a compressional effect for high rotational speeds, analogue to a blower which is counteracting the flow of gas. While reducing the rotational speed the flow resistance is reduced and thereby the pressure drop decreases (Neumann et al., 2017b). By decreasing the rotational speed further, a strong increase in the pressure drop is experienced. One explanation is an additional resistance due to the buildup of liquid in the eye of the rotor. The smaller centrifugal force at the eye of the rotor is not strong enough to discharge the liquid, which is sprayed on the packing. Moreover it can be assumed that the hold-up increases in the packing itself which reduces the free cross sectional area and eventually increases the gas velocity and frictional pressure drop in the packing. This strong increase of pressure drop is followed by a maximum which is usually accompanied by significant entrainment. In this operating condition most of the liquid is discharged through the gas outlet. At this point in the eye of the rotor a phase inversion takes place, large amounts of water build up and gas bubbles vigorously erupt from it. The significant relation between rotational speed and of the pressure drop has been observed by many authors (Singh et al., 1992).

Secondly, the operating window can be determined. In Figure 3 b) the investigated operating ranges are displayed. For a stable operation without entrainment a rotational speed less or equal to the noted value is needed. For high liquid loads of around $327 \text{ m}^3\text{m}^{-2}\text{h}^{-1}$ the increase from a maximum rotational speed from 10 to 20 s^{-1} allows to operate the equipment at a four times higher gas capacity factor at the inner radius, while for operation at low liquid loads of around $80 \text{ m}^3\text{m}^{-2}\text{h}^{-1}$ the rotational speed of 10 s^{-1} is sufficient. It is reasonable to assume at this low loads that higher gas capacity factors than investigated in this work could be realizable in the current setup. The highest stable operating point investigated was at an inner liquid load of $327 \text{ m}^3\text{m}^{-2}\text{h}^{-1}$ and a gas capacity factor of 4 at the inner radius of the packing.

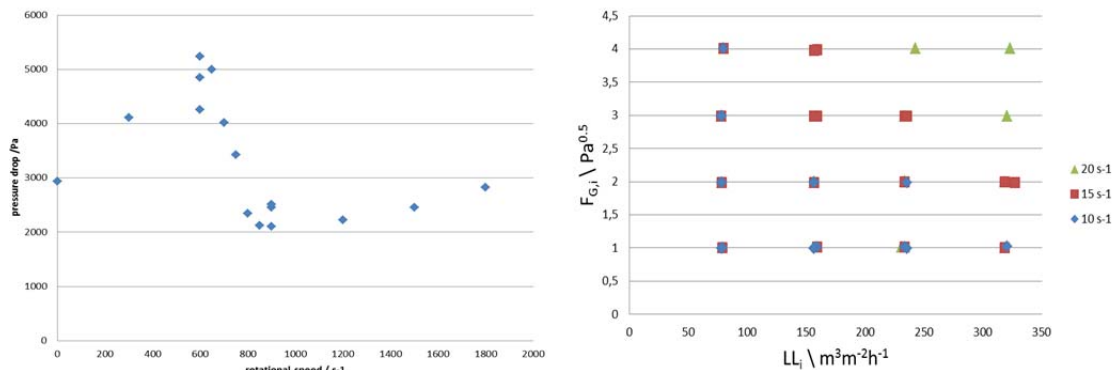


Figure 3: a) shows a typical pressure drop curve for $\dot{V}_L = 0.72 \text{ m}^3\text{h}^{-1}$ [$LL_i = 157 \text{ m}^3\text{m}^{-2}\text{h}^{-1}$] and $\dot{V}_G = 45 \text{ m}_{norm}^3\text{h}^{-1}$ [$F_{G,i} = 3$] b) Shows for different rotational speeds stable operating points at different gas and liquid loads.

For the design of RPB equipment it is important to identify stable operating regions as well as the pressure drop at the specific operating points. The information about the feasible and stable operating regions is important, because it defines the rotational speed selected for the specific application and therefore has an influence on the mechanical design of the machine and the power consumption of the equipment. Additionally the information about the pressure drop in the stable regions dictates the sizing of the auxiliary equipment. Compressors and blowers, which may be installed to overcome certain pressure drops, can significantly add to the investment and operational costs. Moreover, in vacuum applications a high pressure drop can make the process infeasible. In atmospheric pressure applications it offers a new opportunity for readjusting the apparatus for increasing or decreasing capacity. From the hydrodynamic point of view an RPB with a variable speed drive offering 10 to 20 s^{-1} and a design specification of $LL_i 175 \text{ m}^3\text{m}^{-2}\text{h}^{-1}$ and $F_{G,i} 2,5$ would offer at least +/- 60 % capacity flexibility based on the gas flow and -55 % to +85 % based on the liquid load.

The combination of the pressure drop curve and the operating range is illustrated in Figure 4. It shows the pressure drop for all stable experimental points without entrainment at different rotational speeds of 10 s^{-1} (●) and 20 s^{-1} (■). It becomes apparent that higher rotational speed clearly increases the possible operating range. Crossing the bisecting line in the LL_i - $F_{G,i}$ plane seldom stable operating points could be found for rotational speed of 10 s^{-1} at high gas and liquid loads.

Additionally it can be seen that for low gas loads ($F_{G,i} = 1$) the differences in pressure drop for high and low rotational speeds are rather small. For large gas loads ($F_{G,i} = 4$) the pressure drop for a smaller rotational speed can even be higher than for a rotational speed of 20 s^{-1} . This can be explained due to the distance of the operating point to the point where significant entrainment occurs. As shown in Figure 3 a) the pressure drop is exponentially increasing at rotational speeds close to the point of significant entrainment. As a consequence low pressure drop and low rotational speed can be counter acting and need to be simultaneously considered.

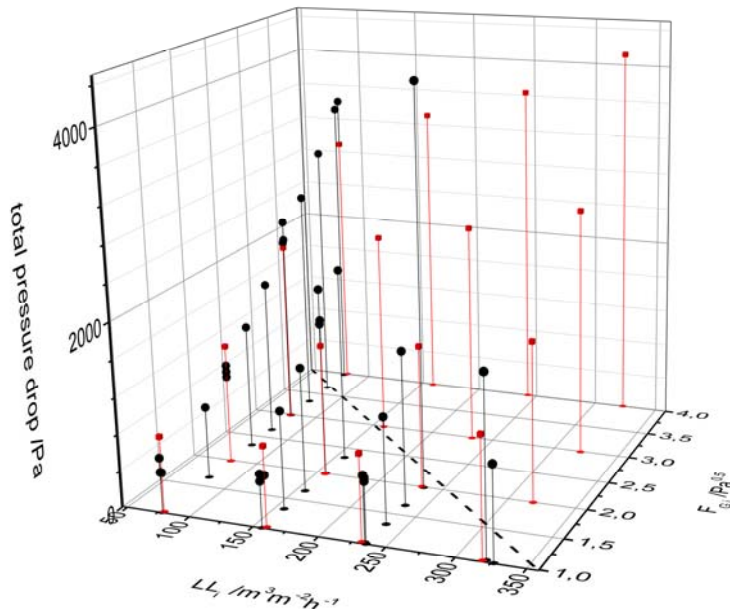


Figure 4: Combination of operating window and pressure drop curve at 10 s^{-1} (●) and 20 s^{-1} (■).

5. Conclusions

The current work showed the hydrodynamic performance of rotating packed beds. High gas and liquid loads up to gas capacity factors of $4 \text{ Pa}^{0.5}$ and liquid loads up to $325 \text{ m}^3 \text{ m}^{-2} \text{ h}^{-1}$ were investigated and stable operating points by varying the rotational speeds for the whole range of investigated operating conditions could be performed. By varying the rotational speed a hydrodynamic capacity increase by a factor of four could be achieved for gas a liquid loads.

Future studies need to investigate the mass transfer performance in the same operating range to validate the feasibility for specific separation tasks in the whole hydrodynamic operating range. Moreover studies elucidating the flow of liquid in the packing could give insights for future packing design and to reduce the pressure drop.

Nomenclature

Latin letters

A_C	cross sectional area	m^2
d	diameter	m
F_G	gas capacity factor	$\text{Pa}^{0.5}$
h	height	m
i	inner	
LL	liquid load	$\text{m}^3 \text{ m}^{-2} \text{ h}^{-1}$
l	length	m
n_{rot}	rotational speed	s^{-1}
r	radius	m
\dot{V}_G	gas volume flow	$\text{m}^3 \text{ h}^{-1}$
\dot{V}_L	liquid volume flow	$\text{m}^3 \text{ h}^{-1}$

Acknowledgments

The support of Christian Haas in conducting the experiments is greatly acknowledged.

The research has been conducted in cooperation with ISPT (Institute for Sustainable Process Technology) within the scope of the project IMPACCT (Improved Process Performance by Process Intensification in Centrifugal Contactors).

References

- Düssel, R., Stichlmair, J., Groebel, M., 2006. Rektifikation, in: Goedecke, R. (Ed.), *Fluidverfahrenstechnik. Grundlagen, Methodik, Technik, Praxis*. Wiley-VCH, Weinheim, pp. 689–798.
- Neumann, K., Hunold, S., Groß, K., Górak, A., 2017a. Experimental investigations on the upper operating limit in rotating packed beds. *Chemical Engineering and Processing: Process Intensification* 121, 240–247. 10.1016/j.cep.2017.09.003.
- Neumann, K., Hunold, S., Skiborowski, M., Górak, A., 2017b. Dry Pressure Drop in Rotating Packed Beds—Systematic Experimental Studies. *Ind. Eng. Chem. Res.* 56 (43), 12395–12405. 10.1021/acs.iecr.7b03203.
- Singh, S.P., Wilson, J.H., Counce, R.M., Lucero, A.J., Reed, G.D., Ashworth, R.A., Elliott, M.G., 1992. Removal of volatile organic compounds from groundwater using a rotary air stripper. *Ind. Eng. Chem. Res.* 31 (2), 574–580. 10.1021/ie00002a019.
- Spiegel, L., Duss, M., 2014. Structured Packings, in: Gorak, A., Olujić, Z. (Eds.), *Distillation*. Elsevier Science, Burlington, pp. 145–181.
- Yildirim, Ö., Flechsig, S., Brinkmann, U., Kenig, E.Y., 2015. Bestimmung der Lastgrenzen konventioneller Strukturpackungen und Anstaupackungen mithilfe des Wallis-Plots. *Chemie Ingenieur Technik* 87 (10), 1348–1356. 10.1002/cite.201500043.